Check for updates

Received: 5 March 2023 | Revised: 14 April 2023 | Accepted: 25 April 2023

DOI: 10.1002/idm2.12106

REVIEW

Interdisciplinary Materials Open Access WILEY

Advances in probing single biomolecules: From DNA bases to glycans

Baofei Hou[1] | Teng Zhang[1] | Huixia Yang[1] | Xu Han[1] | Liwei Liu[1] | Linfei Li[2] | Cesare Grazioli[3] | Xu Wu[1] | Nan Jiang[2] | Yeliang Wang[1]

[1]MIIT Key Laboratory for Low-Dimensional Quantum Structure and Devices, School of Integrated Circuits and Electronics, Beijing Institute of Technology, Beijing, China

[2]Department of Chemistry, University of Illinois Chicago, Chicago, Illinois, USA

[3]IOM-CNR, Istituto Officina dei Materiali, Trieste, Italy

Correspondence

Teng Zhang, Xu Wu, and Yeliang Wang, MIIT Key Laboratory for Low-Dimensional Quantum Structure and Devices, School of Integrated Circuits and Electronics, Beijing Institute of Technology, 100081 Beijing, China.

Email: teng.zhang@bit.edu.cn, xuwu@bit.edu.cn and yeliang.wang@bit.edu.cn

Funding information

Strategic Priority Research Program of Chinese Academy of Sciences, Grant/Award Number: XDB30000000; National Natural Science Foundation of China, Grant/Award Numbers: 92163206, 61971035, 61725107, 62271048; Natural Science Foundation of Beijing Municipality, Grant/Award Numbers: Z190006, 4192054; National Key Research and Development Program of China, Grant/Award Numbers: 2019YFA0308000, 2020YFA0308800, 2021YFA1400100

Abstract

Imaging biomolecules in real space is crucial for gaining a comprehensive understanding of the properties and functions of biological systems at the most fundamental level. Among the various imaging techniques available for biomolecules and their assembled nanostructures, scanning probe microscopy (SPM) provides a powerful and nondestructive imaging option. SPM is unique in visualizing intrinsically disordered biomolecules at the nanometer scale (e.g., glycans). This review highlights recent achievements in studying biomolecules using SPM technique, focusing on DNA bases, amino acids, proteins, and glycans. The atomic-level analysis of biomolecules made possible by SPM allows for a more accurate definition of the local structure–property relationship. High-resolution SPM imaging of single biomolecules offers a new way to study basic processes of life at the molecular level.

KEYWORDS

atomic-scale probing, biomolecules, scanning probe microscopy, structure, visualization

1 | INTRODUCTION

Biomolecules represent the basic building blocks of organisms. The study of biomolecules provides insights into the nature of biomolecular interactions and the mechanisms of many biological processes that form the critical bases for controlling the properties and functions of organisms.[1–3] To that end, it is of primary importance to understand complicated biomolecular structures, which requires a multidisciplinary approach,[4,5] involving analytical chemistry,[6] soft matter physics,[7] and biochemistry.[8] In particular, physics-based experimental observations can facilitate structural analysis and support synthetic chemistry, thereby enhancing the understanding of biomolecules.[9,10] Furthermore, understanding and operating biomolecules are intensively demanded in view of the unique role of biomolecules in life medicine, disease

This is an open access article under the terms of the Creative Commons Attribution License, which permits use, distribution and reproduction in any medium, provided the original work is properly cited.

© 2023 The Authors. *Interdisciplinary Materials* published by Wuhan University of Technology and John Wiley & Sons Australia, Ltd.

treatment, and molecular recognition, as well as their essential status and functions in organisms.

Indeed, structural information on biomolecules, as the primary concern in molecular biology, has attracted considerable attention over the past decades.[11–15] To gain insight into the biomolecular structure and conformations, various imaging techniques have been utilized to achieve this goal.[16–18]

As already discussed in Dufrêne et al.,[19] Transmission Electron Microscopy (TEM) can obtain the structure and conformation of proteins, and the structure of organisms with a molecular resolution. However, the sample used for characterizing by TEM needs drying and depositing on the grid, which can disrupt the biological activity of the molecules during the imaging process. Super-resolution microscopy (STED, PALM, and STORM) can acquire three-dimensional (3D) cell structure and monitor the evolution of living molecules in organisms. However, it should be noted that these imaging techniques are limited to visualizing fluorescence labels. Holographic coherent diffraction is a promising alternative to both TEM and super-resolution microscopy, as it can achieve subnanometer resolution images of individual protein and protein complexes without inducing radiation damage.

On the other hand, scanning probe microscopy (SPM) provides a direct visualization technology with ultrahigh spatial resolution for imaging biomolecules on the subnanometer scale.[19–27] The high-resolution visualization of biomolecular structures also significantly impacts biophysics and biochemistry.[28–31] This kind of visualization is beneficial for revealing important structural information, such as the shape, size, and orientation of biomolecules, which is essential for understanding their function and behavior.

Two widely used branches of SPM, Scanning Tunneling Microscopy (STM) and Atomic Force Microscopy (AFM), offer unprecedented opportunities to study biomolecules.[32–36] STM and AFM can image biomolecules under different conditions without damaging their structures and biological activities, making them ideal for studying delicate biomolecules.

SPM allows for real-time biomolecule imaging, meaning that dynamic processes, such as conformational changes or interactions between biomolecules, can be obtained in situ. This provides valuable insights into the behaviors and functions of biomolecules in their native condition. SPM can provide quantitative measurements of various properties of biomolecules, such as surface roughness, height, elasticity, and electrical conductivity. This allows for characterizing biomolecules and their interactions with other molecules in a quantitative manner, which is important for understanding their functions and properties.

Moreover, SPM allows for manipulating and functionalizing biomolecules at the nanoscale. This capability offers unique opportunities to design and fabricate functional biomolecule-based devices for various applications.

To date, several types of biomolecules have been characterized using SPM, such as proteins, nucleic acids, lipids, carbohydrates, enzymes, and so on.[37,38] In this review, we summarize the substantial progress of STM and AFM in studying biomolecules. As shown in Figure 1, we concentrate on biomolecules, including amino acid, DNA, protein, and glycans by applying multifunctional imaging modes of SPM. Moreover, we introduce a new deposition technique, that is, electrospray ion beam deposition (ES-IBD), and discuss how it can combine with SPM for single-biomolecule studies. Finally, we present the technique's challenges, research trends, and future prospects.

2 | STM AND AFM: A BRIEF INTRODUCTION

Figure 2A shows the working mechanism of STM, where a metallic tip is brought close to the sample to form a tunneling junction between them. Within the tunneling junction, the electron wave function of the tip overlaps with that of the sample. By applying a voltage between the tip and the sample, a tunneling current flows from the tip to the sample or vice versa.[39] The tunneling current is exponentially related to the tip and the sample's integrated local density of states. While the tip scans over the sample surface, a feedback system maintains a constant tunneling current, enabling the morphology of the sample surface to be obtained, and facilitating the realization of the visualization of the sample surface at the atomic scale.[40,41]

AFM is another imaging technique that is usually used to observe various objects in physics and chemistry. Moreover, AFM can also be applied to soft systems, such as synthetic biology and oncology.[19,42–49] Nowadays, many new AFM imaging modes have been developed.[19,33,50–53] Contact mode, the primary imaging mode of AFM, has been widely used for decades.[32,54] However, in contact mode, the lateral forces generated during the scanning process cause reversible or irreversible deformations of soft biological systems.[55] To overcome this issue and maximize the resolution, the researchers in the field developed the frequency-modulated noncontact mode.[56–58] The cantilever oscillates at the resonance frequency in the imaging mode and generates a resonance frequency shift (Δf) when the tip approaches to the sample (Figure 2B).[59] Δf is proportional to the gradient of the interaction force (F_{ts}) in the limit of small

2767441x, 0, Downloaded from https://onlinelibrary.wiley.com/doi/10.1002/idm2.12106 by CNR GROUP II Istituto di Scienza dell', Wiley Online Library on [26/06/2023]. See the Terms and Conditions (https://onlinelibrary.wiley.com/terms-and-conditions) on Wiley Online Library for rules of use; OA articles are governed by the applicable Creative Commons License

FIGURE 1 This review concentrates on the study of DNA self-assembly, DNA molecules, amino acids, proteins, and glycans (pentamannoside and hexamannoside) by the SPM technique. SPM, scanning probe microscopy.

amplitudes, allowing high-resolution contouring of biological samples.[32]

3 | SPM STUDY ON DNA AND ITS COMPOSITION

DNA is a complex molecule that stores genetic information in organisms. To acquire knowledge of the structures and conformations of DNA molecules, SPM has been used to study DNA and its composition in different conditions, providing valuable insights into its structural and conformational properties. In the following, we will give some notable examples and achievements of SPM in studying DNA and its composition.

3.1 | Imaging single DNA molecules

Imaging DNA molecules is a challenge due to the requirement for high spatial resolution and accuracy. SPM can image a single DNA molecule in real space owing to the imaging capacity at the atomic level. Moreover, SPM exhibits excellent environmental compatibility, allowing for investigating biomolecules in various conditions, ranging from solutions to ambient conditions and ultrahigh vacuum environments.[60–62] Cricenti et al. used STM to study double-stranded DNA in the air for the first time, revealing its helical conformation (Figure 3A).[63] Pawlak et al. characterized single-strand DNA (ssDNA) conformations by STM down to the subnanometer scale.[64] They found that

2767441x, 0, Downloaded from https://onlinelibrary.wiley.com/doi/10.1002/idm2.12106 by CNR GROUP II Istituto di Scienza dell', Wiley Online Library on [26/06/2023]. See the Terms and Conditions (https://onlinelibrary.wiley.com/terms-and-conditions) on Wiley Online Library for rules of use; OA articles are governed by the applicable Creative Commons License

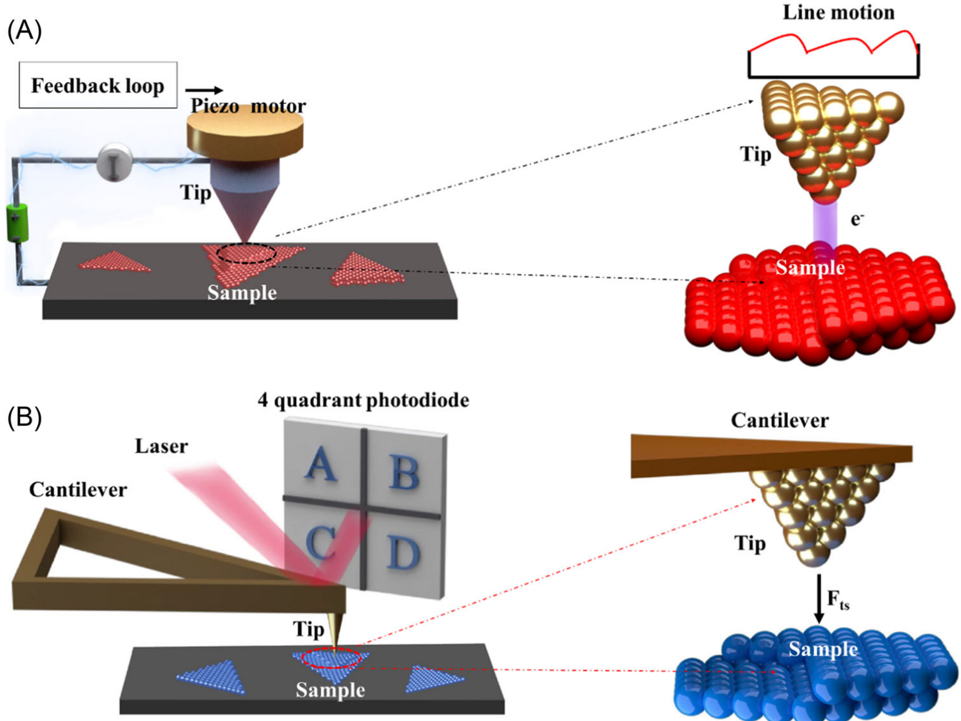

FIGURE 2 Schematic diagram illustrating the typical setup of (A) Scanning Tunneling Microscopy (STM) and (B) Atomic Force Microscopy (AFM). In STM, a bias voltage V is applied between the tip and the sample, while the tip scans the surface in the *xy*-plane. The *z* coordinate of the tip is adjusted using a three-dimensional piezoelectric scanner controlled by a feedback loop. In AFM, a laser light is reflected off the back of the tip onto the photodiode. The deflection of the cantilever is measured as it tracks the surface, enabling the acquisition of an image depicting the sample topography. Both STM and AFM utilize feedback electronics to regulate the tip–sample separation.

the hydrated ssDNA can transform into dehydrated ssDNA oligomers (Figure 3B,C) at a sample annealing temperature of 440 K, and linear structures with a length of several nanometers emerged as the temperature increased (Figure 3D), suggesting the diverse structural nature of ssDNA in real space.

Tanaka and Kawai used STM to sequence individual guanine bases in single-stranded DNA molecules to investigate single DNA further.[65] The single base appears as bright protrusions in the STM topography image (Figure 3E) and *DI*/*dV* mapping (Figure 3F), which is perfectly matched with a part of the known guanine base sequence of M13mp18 of viral DNA molecules (Figure 3G). Moreover, they also identified the adenine base of the extended M13mp18. As shown in Figure 3H, white and yellow characters represent guanine and adenine sites, respectively.[66] Unlike guanine, adenine has no distinct contrast in the topographic image.

AFM was used to get the details of a single DNA.[68–70] Among the different working models of AFM, Frequency Modulation AFM (FM-AFM) was widely applied to investigate plasmid DNA in an aqueous solution.[20] The major and minor grooves (partly marked by red and blue arrows) of double helix structure DNA with different widths were resolved (Figure 3I,J). The conformations of two polynucleotide chains in a single DNA double helix were also observed in near-physiological conditions.[67] The DNA appears as a tilted right-handed double helix structure (Figure 3K), while the DNA with an elongated helical conformation is a left-handed double helix (Figure 3L).

In short, the direct imaging of DNA molecules at the submolecule scale by SPM holds promise for establishing the structure–function relationship of biomolecular systems in vivo with high resolution.

3.2 | Imaging the self-assembled patterns of DNA bases

Studying the self-assembly of complementary DNA bases, such as guanine (G), cytosine (C), adenine (A), and thymine (T), is essential to understand DNA structures comprehensively.[71,72] A well-ordered assembled structure formed by Watson-Crick G–C pairs at a liquid/solid interface was investigated.[73] The molecular rows and

2767441x, 0, Downloaded from https://onlinelibrary.wiley.com/doi/10.1002/idm2.12106 by CNR GROUP II Istituto di Scienza dell', Wiley Online Library on [26/06/2023]. See the Terms and Conditions (https://onlinelibrary.wiley.com/terms-and-conditions) on Wiley Online Library for rules of use; OA articles are governed by the applicable Creative Commons License

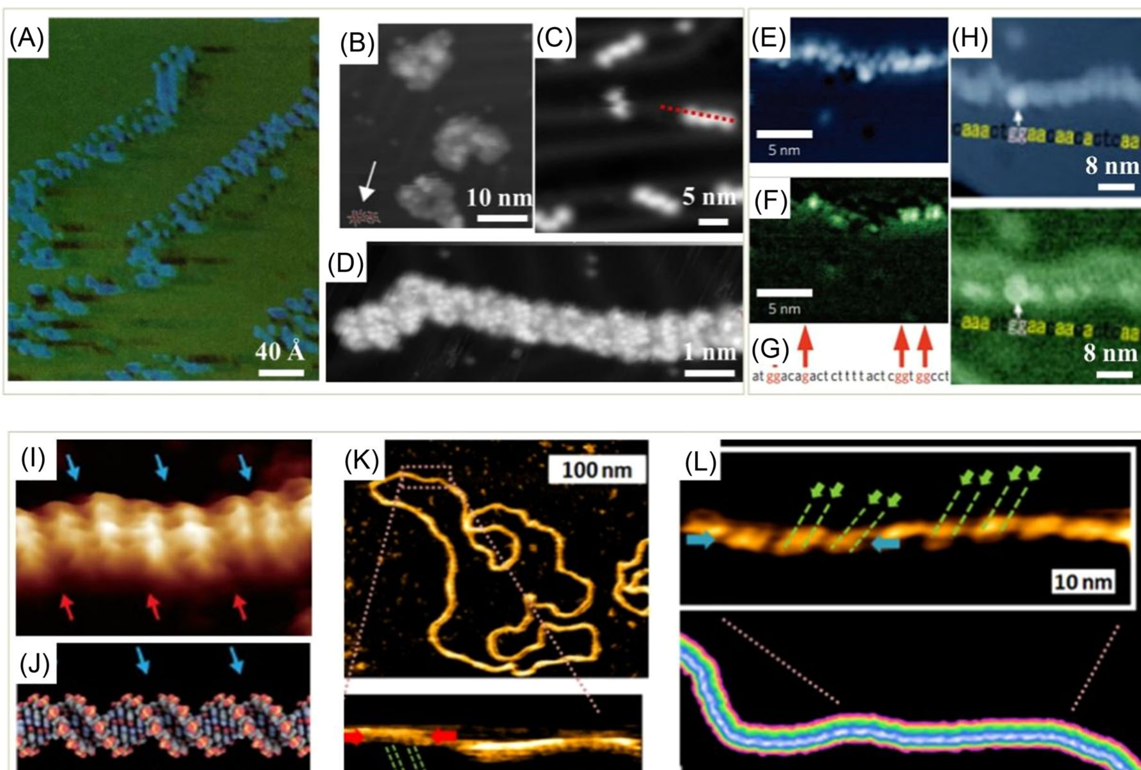

FIGURE 3 Imaging nucleotides and single DNA chains. (A) $d(\ln I)/ds$ image of DNA molecules on Au. (B–D) STM images of hydrated, dehydrated, and self-assembled cytosine single-strand DNA. (E–G) STM images of single-stranded M13mp18 DNA molecules and part of the base sequence of M13mp18 from a databank. (H) STM analysis of single-stranded M13mp18 DNA molecules. (I, J) FM-AFM topographic image and molecular structure of the double helix plasmid DNA. (K, L) High-resolution AFM images of two polynucleotide chains in the DNA double helix. (A) is reproduced with permission from Cricenti et al.,[63] Copyright Science, 1989. (B)–(D) are reproduced with permission from Pawlak et al., [64] Copyright Springer Nature, 2019. (E)–(G) are reproduced with permission from Tanaka and Kawai,[65] Copyright Macmillan Publishers Limited, 2009. (H) is reproduced with permission from Tanaka and Taniguchi,[66] Copyright The Japan Society of Applied Physics, 2017. (I) and (J) are reproduced with permission from Ido et al.,[20] Copyright American Chemical Society, 2013. (K) and (L) are reproduced with permission from Leung et al.,[67] Copyright American Chemical Society, 2012. FM-AFM, Frequency Modulation Atomic Force Microscopy; STM, Scanning Tunneling Microscopy.

quasisquare arrangement features are prominent for pure C and G, respectively (Figure 4A,B). However, a distinct double-row structure is formed during the coadsorption of G and C (Figure 4C), ascribing to the alignment by the hydrogen-bonded GC dimers.

Besides the above-mentioned liquid/solid interfaces, the self-assembly of complementary DNA bases (A and T) was also observed on a solid surface.[74] Every two A molecules pack as A–A dimers (indicated with yellow bars) and form a stable 2D network (Figure 4D). Each T molecule is hydrogen-bonded to two neighbors, leading to T–T dimers and a "zigzag" structure (Figure 4E). A well-ordered cyclic structure was also observed by mixing A and T molecules at a specific molar ratio (Figure 4F).

The reversible assembly/reassembly process between guanine motifs was also observed to study the self-assembly of DNA bases systemically.[75] The alternation of the guanine ribbon (Figure 4G) and the guanine quartet (Figure 4H) was achieved by adding potassium picrate ($K^+(pic)^-$) to the guanine ribbon or adding cryptand to the guanine quartet, indicating that guanine molecules can reversibly interconvert between two motifs.

Furthermore, the hydration process of DNA bases was explored to enhance the comprehension of the self-assembly of DNA bases.[76] The controllable interconversion between adenine–H_2O complexes and adenine was realized by adding or removing water molecules (Figure 4I), resulting in a controllable scission or stitching of the adenine structure.

Observing the self-assembly of complementary DNA bases at different conditions provides new insights into the formation of early biological macromolecules, intending to inspire further research to reveal life processes.

2767441x, 0, Downloaded from https://onlinelibrary.wiley.com/doi/10.1002/idm2.12106 by CNR GROUP II Istituto di Scienza dell', Wiley Online Library on [26/06/2023]. See the Terms and Conditions (https://onlinelibrary.wiley.com/terms-and-conditions) on Wiley Online Library for rules of use; OA articles are governed by the applicable Creative Commons License

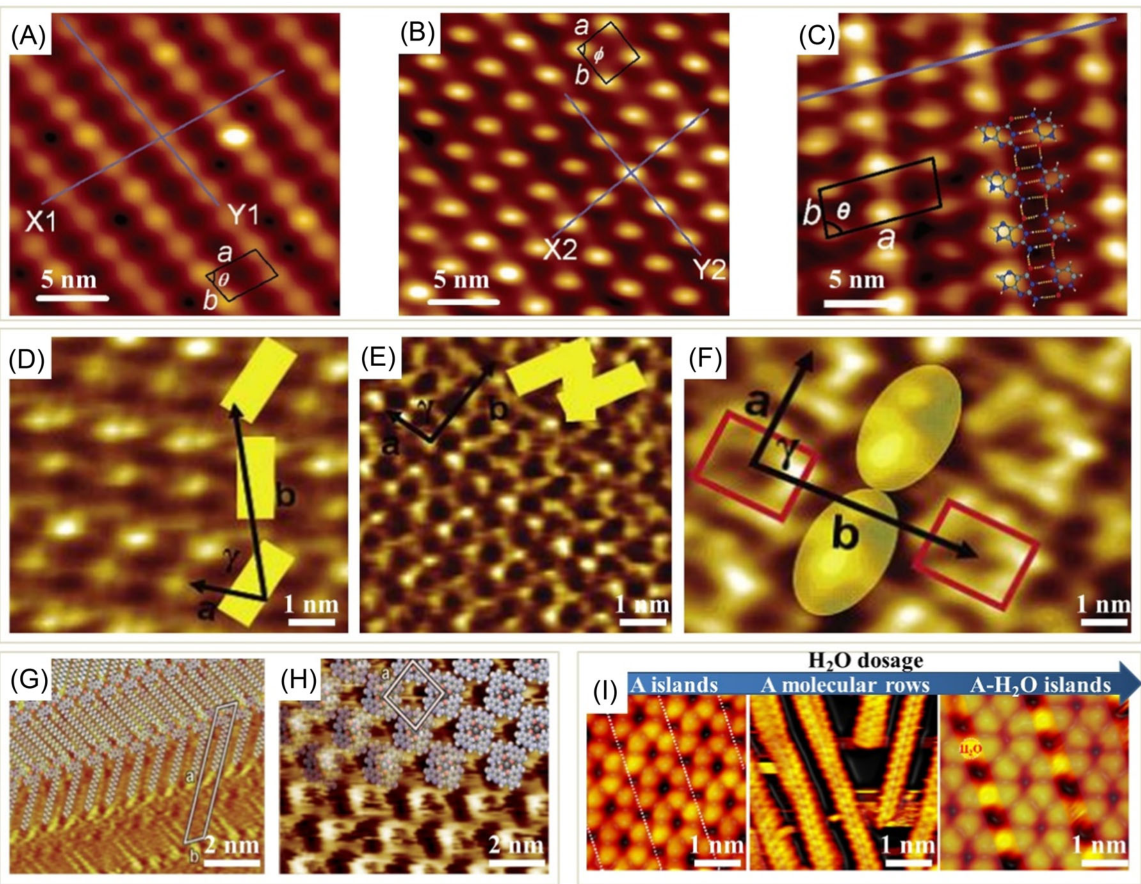

FIGURE 4 Imaging of DNA bases self-assembly. (A–C) STM images of cytosine, guanine, and coadsorption of guanine and cytosine. (D–F) STM images of adenine, thymine, and the mixture of adenine and thymine. (G, H) STM images of guanine ribbon and guanine quartet. (I) Dynamic hydration process of adenine molecular and adenine–H_2O. (A)–(C) are reproduced with permission from Xu et al.,[73] Copyright American Chemical Society, 2006. (D)–(F) are reproduced with permission from Mamdouh et al.,[74] Copyright American Chemical Society, 2006. (G) and (H) are reproduced with permission from Ciesielski et al.,[75] Copyright Wiley-VCH Verlag GmbH & Co. KGaA, Weinheim, 2010. (I) is reproduced with permission from Zhang et al.,[76] Copyright The Royal Society of Chemistry, 2018. STM, Scanning Tunneling Microscopy.

4 | CHARACTERIZING AMINO ACIDS AND PEPTIDES/PROTEINS

Amino acids are the foundational building blocks of proteins and participate in numerous essential biological processes. To get the details of amino acids, SPM was utilized to investigate various types of amino acids and achieved some achievements. Peptides and proteins, larger biological molecules made up of amino acid chains were also studied to gain insight into the structures and functions of biomolecules.

4.1 | Imaging single amino acids

Amino acids, the basic unit of proteins, participate in many essential life activities, such as metabolism.[77,78] Visualizing single amino acids is vital for gaining a fundamental understanding of their interaction. The self-assembly structure of amino acids (R- and S-alanine) on Cu(110) was studied.[79] A typical STM image is shown in Figure 5A, where each bright protuberance represents an alanine molecule, and six or eight molecules are arranged in pairs to form a cluster. The adsorption and self-assembly of glutamic acid on Ag(100) were investigated to further understand single amino acids.[80] Different structures, such as flower- and square-like structures, are shown in Figure 5B.[81]

Forster et al. studied proline molecules on Cu(110) to gain deeper insight into amino acids.[82] A (4×2) overlayer was observed following the deposition of enantiopure (S)-proline on Cu(110) (Figure 5C). Two different conformations, that is, conformer A and conformer B, are formed due to different bonds of proline

2767441x, 0, Downloaded from https://onlinelibrary.wiley.com/doi/10.1002/idm2.12106 by CNR GROUP II Istituto di Scienza dell', Wiley Online Library on [26/06/2023]. See the Terms and Conditions (https://onlinelibrary.wiley.com/terms-and-conditions) on Wiley Online Library for rules of use; OA articles are governed by the applicable Creative Commons License

2767441x, 0, Downloaded from https://onlinelibrary.wiley.com/doi/10.1002/idm2.12106 by CNR GROUP II Istituto di Scienza dell', Wiley Online Library on [26/06/2023]. See the Terms and Conditions (https://onlinelibrary.wiley.com/terms-and-conditions) on Wiley Online Library for rules of use; OA articles are governed by the applicable Creative Commons License

FIGURE 5 Characterization of single amino acid self-assembly by STM and AFM. (A) High-resolution STM image of S-alanine on Cu (110). (B) AFM images of (S)-glutamic acid absorbed on Ag(100). (C, D) STM image of (S)-proline on Cu(110) and two different conformers formed by proline and copper atom. (A) is reproduced with permission from Xu et al.,[79] Copyright The Royal Society of Chemistry, 2011. (B) is reproduced with permission from Tranca et al.,[81] Copyright American Chemical Society, 2013. (C) and (D) are reproduced with permission from Forster et al.,[82] Copyright Wiley-VCH Verlag GmbH & Co. KGaA, Weinheim, 2010. AFM, Atomic Force Microscopy; DFT, density functional theory; STM, Scanning Tunneling Microscopy.

and copper atoms. Conformer A forms a bright protrusion, while conformer B appears as a faint protrusion (Figure 5D), indicating that single-molecule studies can distinguish the adsorption footprints formed by amino acids.

In brief, investigating the unique arrangements of amino acids is a powerful approach to deepen our comprehension of how amino acids interact and provide insights into the conformation of diverse biomolecules.

4.2 | Imaging folded peptides/proteins

Peptides/proteins have been studied to gain a comprehensive understanding of the structures and functions of biomolecules. For instance, the chirality of the self-assembled nanofibers with short amphiphilic peptides was investigated.[83] The fibril formed by $^{L}I_3{}^{L}K$ shows a twisted left-handed conformation (Figure 6A). In contrast, its enantiomer $^{D}I_3{}^{D}K$ comprises a right-handed twisted conformation (Figure 6B), indicating that the chirality of constituent amino acids plays a crucial role in controlling their morphological handedness. Furthermore, the self-assembly of peptides was explored to create chiral nanostructures by changing the amino acid sequence.[84] Right-handed helical nanofiber can be formed by self-assembling 9-fluorenylmethoxycarbonyl (Fmoc)-FWH tripeptide (Figure 6C). In contrast, left-handed nano helices would be formed when the intermediate amino acid Trp (W) in Fmoc-FWH tripeptide is replaced by Phe (Figure 6D), indicating that the change of amino acids sequence can alter the chirality of tripeptides.

Dynamic information of proteins is vital for understanding and manipulating biomolecules. Myosin

V, a protein found in most animal genomes, was studied by high-speed AFM.[85] The hand-over-hand movement of tail-truncated myosin V in a short interval of microseconds can be obtained and is presented in Figure 6E–H.

The electron transfer process in proteins, which plays a crucial role in photosynthesis and enzymatic reactions, was studied to gain insight into protein functions.[86] Figure 6I,J demonstrates the self-assembled long-axis and short-axis cytochrome b_{562} protein molecules in two different orientations on the Au(111) surface. Notably, these two types of molecules are well-dispersed on the surface (Figure 6K,L), and the function of the cytochrome b_{562} protein can be retained when it is absorbed onto the Au(111) surface.

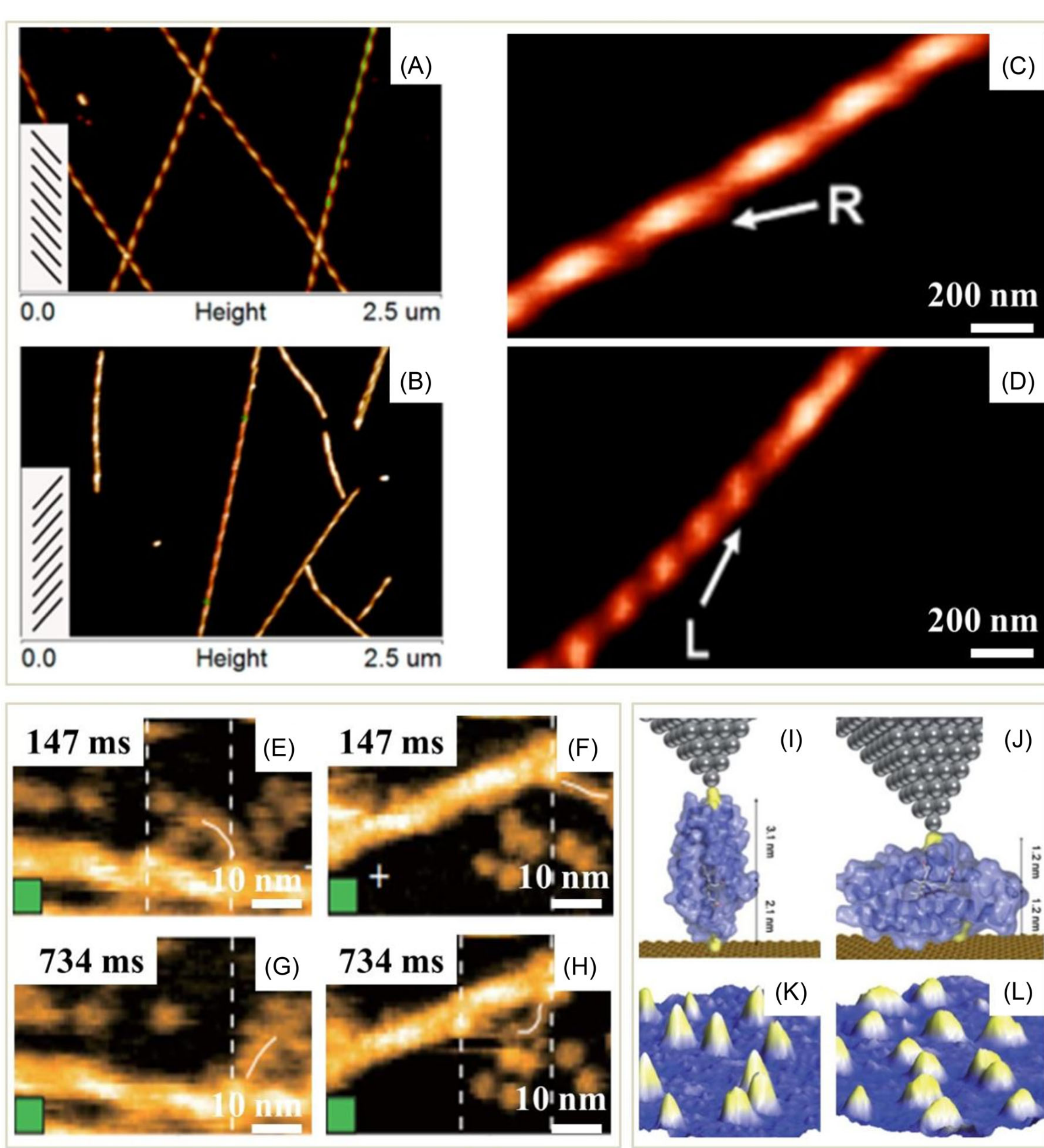

FIGURE 6 Observation of single peptides/proteins. (A, B) AFM images of amphiphilic peptides ${}^{L}I_3{}^{L}K$ and ${}^{D}I_3{}^{D}K$ fibrils. (C, D) AFM images of right-handed and left-handed helical nanofibers formed by fluorenylmethox ycarbonyl-tripeptide. (E–H) AFM images of tail-truncated myosin V undergoing hand-over-hand movement. (I–L) Schematic and STM images of long-axis configuration (left) and short-axis configuration protein cytochrome b_{562} (right). (A) and (B) are reproduced with permission from Wang et al.,[83] Copyright American Chemical Society, 2017. (C) and (D) are reproduced with permission from Xing et al.,[84] Copyright American Chemical Society, 2018. (E)–(H) are reproduced with permission from Kodera et al.,[85] Copyright Macmillan Publishers Limited, 2010. (I)–(L) are reproduced with permission from Della Pia et al.,[86] Copyright The Royal Society of Chemistry, 2012. AFM, Atomic Force Microscopy; STM, Scanning Tunneling Microscopy.

2767441x, 0, Downloaded from https://onlinelibrary.wiley.com/doi/10.1002/idm2.12106 by CNR GROUP II Istituto di Scienza dell', Wiley Online Library on [26/06/2023]. See the Terms and Conditions (https://onlinelibrary.wiley.com/terms-and-conditions) on Wiley Online Library for rules of use; OA articles are governed by the applicable Creative Commons License

The observation of proteins/peptides using SPM can yield valuable information regarding structural biology and single-molecule dynamics, providing essential references for the preservation of molecular biological functions.

4.3 | Imaging peptides/proteins self-assembly

The self-assembly of peptides, a vital link in protein formation, has attracted attention in the past decades.[87–91] For example, the self-assembly of the tetrapeptides KFFE and KVVE was studied.[92] Figure 7A shows the island-like structure of KFFE with a parallel-row arrangement formed by double protuberances, depicted by solid and dashed lines representing two types of row boundaries. The peptide unit cell is marked by white oval contours. The antiparallel structure of the rotor-shaped KVVE is illustrated in Figure 7B with white outlines. The different combinations of conformations originate from the intramolecular, intermolecular, and different rows of adjacent residues (Figure 7C). These findings have paved the way for designing novel self-assembled peptide structures using techniques such as molecular deposition in a vacuum.

The chiral recognition of di-phenylalanine was explored to get peptides' information.[93] The supramolecular chirality generated by the stereoselective self-assembly of two or more dipeptides in the homochiral chain is depicted (Figure 7D). The high-resolution STM images of isolated di-L-phenylalanine and di-L-phenylalanine are obtained (Figure 7E,F). The dynamic process of conformation adjustment is also obtained by STM images and density functional theory (DFT) calculations, revealing the "induced fit" mechanism at the single-molecule level.[95]

The utilization of two oligopeptides with only two amino acid differences as bio-organic building blocks for 2D self-assembly was demonstrated, resulting in sequence-controlled molecular nanostructures.[24] Two types of ordered assemblies are observed when decapeptide angiotensin I is deposited on Au(111) surface. Structure A consisting of chains with staggered dimers can be ascribed to two peptides aligned in an antiparallel manner (Figure 7G). A more compact assembly named structure B is formed, in which the molecules are stacked parallel along the long side, resulting in rows with alternating contrast at the interface of rows. Instead of small assemblies, extended domains of chiral honeycomb networks with large hexagonal pores can be observed for angiotensin II molecules (Figure 7H).

In addition, Chen et al. designed the conjugated macrocycle (CPN8) supramolecular nanopores to manipulate antibiotic peptide (valinomycin).[96] The valinomycin with three lobes located in the cavity of CPN8 can be clearly observed. To further understand valinomycin, STM was employed to investigate the K^+-induced switching of valinomycin.[94] The 3D image of one valinomycin molecule scattered in the macrocycle is presented. The white arrow indicates the triangle-shaped valinomycin (Figure 7I). A structural model for the product formed by cyclic arylamide and valinomycin is proposed based on STM imaging (Figure 7J).

To address the issues of complex biological systems, AFM was also performed to study the self-assembly of peptides/proteins.[44,97–99] The short dodecapeptide selected by phages can self-assemble on graphite and form long-range ordered nanostructures.[100] The peptide self-assembly process can be divided into surface aggregation, gradual densification, and ordering, similar to epitaxial growth processes of atomic systems on surfaces. Thus, imaging the self-assembly of peptides can improve the understanding of peptides' information.[101,102]

5 | IMAGING GLYCANS

Glycans serve as both structural scaffolds and sources of chemical energy in the cells of organisms. However, the development of carbohydrate-based research has been limited by challenges in preparing these molecules. To overcome these obstacles, researchers in the field developed ES-IBD to prepare macromolecules and large nonvolatile molecules. ES-IBD has been integrated with SPM to facilitate detailed investigations of the structure and properties of glycans.

5.1 | Schematic workflow of ES-IBD

Considerable progress has been made in molecular biology to date.[103–105] However, its further development is hindered due to the limitations of preparing macromolecules and large nonvolatile molecules.[106–109] To meet the requirement for the development of molecular biology, ES-IBD is developed, which can effectively deposit macromolecule and nonvolatile molecules on a predetermined interface and functionalize surfaces by controlling deposition parameters.[110–115] The schematic workflow of ES-IBD is demonstrated in Figure 8,[28] where the quadrupole mass-to-charge ratio (m/z) filter and the time-of-flight mass spectrometer purify and monitor the molecular ion beam. The electrostatic lenses are applied to

27674lx, 0, Downloaded from https://onlinelibrary.wiley.com/doi/10.1002/idm2.12106 by CNR GROUP II Istituto di Scienza dell', Wiley Online Library on [26/06/2023]. See the Terms and Conditions (https://onlinelibrary.wiley.com/terms-and-conditions) on Wiley Online Library for rules of use; OA articles are governed by the applicable Creative Commons License

FIGURE 7 Exploration of self-assembly of protein/peptide. (A–C) STM images of tetrapeptides KFFE and KVVE. (D–F) STM images of di-D-phenylalanine and its enantiomer. (G, H) STM images of the staggering chains assembly and well-ordered honeycomb network of angiotensin II on Au(111). (I, J) 3D STM image and structure model of cyclo[16]aramide and valinomycin. (A)–(C) are reproduced with permission from Kalashnyk et al.,[92] Copyright American Chemical Society, 2012. (D)–(F) are reproduced with permission from Lingenfelder et al.,[93] Copyright Wiley-VCH Verlag GmbH & Co. KGaA, Weinheim, 2007. (G) and (H) are reproduced with permission from Abb et al.,[24] Copyright Springer Nature, 2016. (I) and (J) are reproduced with permission from Li et al.,[94] Copyright The Royal Society of Chemistry, 2013. STM, Scanning Tunneling Microscopy.

put the beam selected by the m/z filter on the surface. The ion current on the sample is measured during the deposition, while its integration yields the deposited charge. Such charges can be converted to molecular coverage for a defined deposition area. The desired coverage can be obtained with high precision by simply switching off the ion beam once a specific charge is reached. Moreover, the sample can be transferred in situ to the STM system for further characterization after the deposition.

5.2 | Real-space visualization of glycans by STM/ES-IBD

Carbohydrates, also known as saccharides, serve as the structural scaffolds and sources of chemical energy within the cells of organisms and are ubiquitous in nature.[12,116–120] The self-assembly and conformation of Trehalose, a nonreducing disaccharide with polymorphic and anhydrobiotic properties,[121–123] on Cu(100) surface were explored by combining STM/ES-IBD and multistage

2767441x, 0, Downloaded from https://onlinelibrary.wiley.com/doi/10.1002/idm2.12106 by CNR GROUP II Istituto di Scienza dell', Wiley Online Library on [26/06/2023]. See the Terms and Conditions (https://onlinelibrary.wiley.com/terms-and-conditions) on Wiley Online Library for rules of use; OA articles are governed by the applicable Creative Commons License

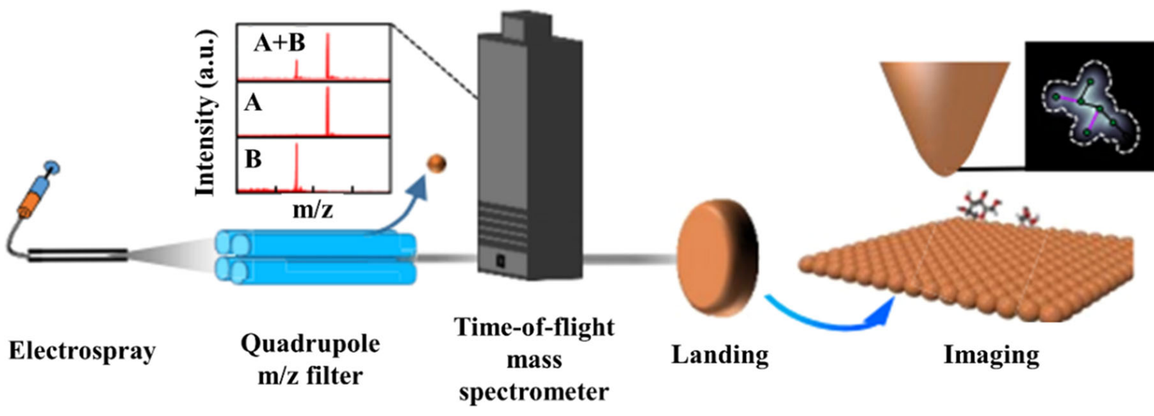

FIGURE 8 Schematic workflow of the electrospray ion beam deposition. Reproduced with permission from Wu et al.,[28] Copyright Springer Nature, 2020.

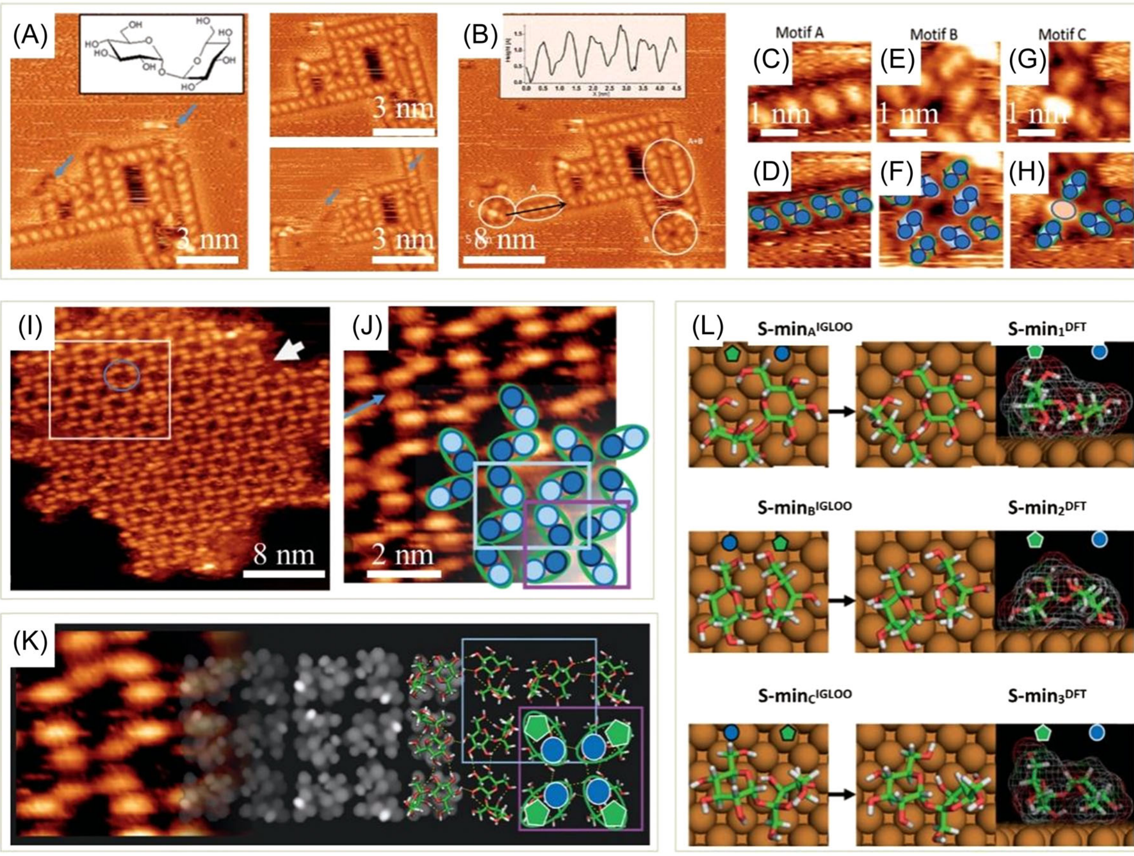

FIGURE 9 Preparation and exploration of the carbohydrate self-assembly by STM/ES-IBD. (A–H) Time evolution and three ordered motifs A–C of trehalose. (I–L) Self-assembly and models of sucrose. (A)–(H) are reproduced with permission from Abb et al.,[124] Copyright The Royal Society of Chemistry, 2019. (I)–(L) are reproduced with permission from Abb et al.,[125] Copyright Die Autoren. Verçffentlicht von Wiley-VCH Verlag GmbH & Co. KGaA, Weinheim, 2019. ES-IBD, electrospray ion beam deposition; STM, Scanning Tunneling Microscopy.

modeling approach.[124] Figure 9A records the rearrangement and alteration of trehalose assemblies with time evolution, showing the mobility of the molecules. Three distinct motifs (motifs A–C) are observed during the trehalose molecules' self-assembly process (Figure 9B). Figure 9C exhibits anisotropic assembly, where the single trehalose molecules and the two saccharide subunits are labeled with green lobes and two blue circles, respectively (Figure 9D). Motif B depicts a square arrangement consisting of eight molecules (Figure 9E), where a

2767441x, 0, Downloaded from https://onlinelibrary.wiley.com/doi/10.1002/idm2.12106 by CNR GROUP II Istituto di Scienza dell', Wiley Online Library on [26/06/2023]. See the Terms and Conditions (https://onlinelibrary.wiley.com/terms-and-conditions) on Wiley Online Library for rules of use; OA articles are governed by the applicable Creative Commons License

windmill-like pattern is formed by four molecules (marked by blue), and the four remaining molecules are located at the corners (green outline), aligning with adjacent molecules (Figure 9F). The bright central feature of motif C consists of one or two bright spots plus several molecules (Figure 9G,H). The individual trehalose molecule is identified by combining STM images and multistage modeling approach simulations. These results demonstrate a new technique's feasibility by combining ES-IBD and STM, for surface assemblies and high-resolution imaging, respectively. The combined technique serves as a universal method to characterize the complex patterns of nonvolatile molecular species.

Moreover, the combination of ES-IBD, STM, and multistage modeling approach was also applied to shed light on the conformation and assembly of sucrose.[125] As displayed in Figure 9I, almost all molecules are assembled into a periodic porous network comprised of slender double lobes and form 2D islands. Every four lobes come together to form a node (marked by blue circles), and each double lobe corresponds to a single molecule based on its length and width. The high-resolution STM image illustrates that each double lobe is composed of two different circular features, representing two different monosaccharide structural units of sucrose (Figure 9J).

A multistage modeling approach was performed to simulate the sucrose and to further clarify the molecular conformation and interactions. Three types of conformations of a single sucrose molecule were acquired by global exploration and local optimization, and further optimized with DFT calculations (Figure 9K). The configuration of S-min_1^{DFT} illustrates that the fructose ring is upright, while the glucose is almost flat. The configuration of S-min_2^{DFT} presents a bowl-like structure formed by bent molecules. The glucose unit in s-min_3^{DFT} is inclined, while the fructose unit is almost upright.

To determine the ultimate conformation of sucrose on the Cu(100) surface, a simulation of STM image based on the theoretical model of the s-min_3^{DFT} model was implemented (Figure 9L). The intensity distribution on the single molecule demonstrates a good agreement with the STM image, where glucose can be clearly distinguished from fructose by the concave boundary and the brightest feature is the fructose building block. Studying sucrose by combining the ES-IBD-STM-modeling approach lays the foundation for understanding polysaccharide conformations at the submolecular level.

5.3 | Imaging single glycans

Glycan has attracted tremendous attention as a large biomolecule with more diverse and branched structures than peptides and nucleotides.[12,126–128] To acquire the details of glycans at the single-molecule level, real-space imaging of a single molecule is indispensable. Cold ES-IBD was applied to prepare a single glycan in virtue of its capability of reducing surface impurities and accurately controlled deposition on the predetermined surface.[28,29,107] The linear glycans, named α1–6 pentamannoside containing an alkylamino linker group at the reducing terminus, were used for initial imaging experiments. As shown in Figure 10A, five topographic protrusions are observed, which can be resolved as single monosaccharide subunits. The heights of the individual monosaccharide features in glycans are different and clearly separated by local minima (Figure 10B).

To distinguish isomers with different connectivity in glycans, STM directly identifies two-branched hexamannosides. The STM image of hexamannoside 4 shows two side chains branching out at angles close to 90° on the opposite sides of the linear backbone (Figure 10C). In comparison, a more compact shape was observed for hexamannoside 5 due to the greater flexibility (Figure 10D). Subsequently, this method studies the more complex glycans, such as the triply branched undecasaccharide 6. Each monosaccharide subunit is visible because all branches are separated from each other. D1 and D2 + D3 arms can be distinguished according to the number of mannose units (Figure 10E). Direct visualization of the glycan at the single-molecule level under cryogenic conditions allows one to understand biomolecular superstructure and even crack the "sugar code."[129]

To further understand the properties of glycans, the conformation of oligosaccharides is revealed by analyzing the ground and excited conformations produced by the soft collision of oligosaccharides to a surface.[2] The STM image of the adsorbed cellohexaose appears as a chain containing six protrusions, corresponding to six glucose (Glu) units in cellohexaose (Figure 10F–I). The extended, partially coiled, and fully coiled conformers as representative types of conformers are revealed. The horizontal "H" and the vertical "V" orientation states of the Glu units in cellohexaose are also observed.

Moreover, based on the number of V units in the cellohexaose chain, the conformers are grouped to get a reasonable cellohexaose conformational space (Figure 10J–W). VV, VH, HV, or HH linkages are determined by the orientation of one pyranose ring regarding the neighboring ring. HH linkage straightened the chain to form the extended conformer (Figure 10J), while the VV bent the chain by ~60° to produce a coiled conformer (Figure 10W). The diverse conformations illustrate that the geometric freedom of the chain is increased by HV and VH linkages (Figure 10K–V). DFT calculations show that the

2767441x, 0, Downloaded from https://onlinelibrary.wiley.com/doi/10.1002/idm2.12106 by CNR GROUP II Istituto di Scienza dell', Wiley Online Library on [26/06/2023]. See the Terms and Conditions (https://onlinelibrary.wiley.com/terms-and-conditions) on Wiley Online Library for rules of use; OA articles are governed by the applicable Creative Commons License

2767441x, 0, Downloaded from https://onlinelibrary.wiley.com/doi/10.1002/idm2.12106 by CNR GROUP II Istituto di Scienza dell', Wiley Online Library on [26/06/2023]. See the Terms and Conditions (https://onlinelibrary.wiley.com/terms-and-conditions) on Wiley Online Library for rules of use; OA articles are governed by the applicable Creative Commons License

FIGURE 10 Nonaveraged imaging of single glycan molecules. (A–E) STM images of different types of glycans. (F–W) STM images and real-space conformations of cellohexaose. (A)–(E) are reproduced with permission from reproduced from Wu et al.,[28] Copyright Springer Nature, 2020. (F)–(W) are reproduced with permission from Anggara et al.,[2] Copyright American Chemical Society, 2020. STM, Scanning Tunneling Microscopy.

partially coiled and the fully coiled are excited conformation states, while the extended one is the ground conformation state. The conformational landscape of cellohexaose demonstrates that molecular interactions play a central role in biological[130,131] and chemical reactions.[132]

6 | CONCLUSION AND PERSPECTIVES

The identification of biomolecular structures is a fundamental issue in molecular biology. Imaging biomolecules in real space provides essential information for the further analysis of biosystem behaviors and functions. SPM is a powerful imaging technique that enables the characterization of biomolecules at the subnanometer scale, and it can be applied to study biomolecules in solutions and other conditions. SPM-related probing and controlling techniques offer a new pathway for the precise structural manipulation of biomolecules. Nonetheless, there are still challenges in probing biomolecules using SPM. These difficulties primarily arise from issues with sample preparation, imaging in solution, tip–sample interactions, and resolution.

The application of SPM could be extended in several ways in the future. Improving spatial, energy, and temporal resolution, along with optimizing environmental compatibility, are critical for the optimal performance of SPM. Improved spatial and energy resolution, for instance, can be achieved by using molecularly modified tips, which can better replicate the morphological characteristics of 3D biomolecules, facilitating detailed characterization of molecular structure. High-speed imaging can enhance experimental efficiency and facilitate real-time monitoring of molecular interactions. Furthermore, a shorter interaction time between molecules and the tip can better preserve the intrinsic properties of samples. In addition, the integration of SPM with other techniques, such as

ES-IBD, spectroscopy, and microscopy, can provide a more comprehensive analysis of biomolecules.

On the other hand, although the combination of ES-IBD and STM offers a practical and feasible approach for the deposition and characterization of nonvolatile molecules and macromolecules at a single molecular level, the commercialization of this technology still largely hinges on the development of intense ion sources. Therefore, the development of an intense and efficient ion source is necessary for expanding the range of applications of ES-IBD. Combining this technique with a synchrotron source or low-energy electron holography with ES-IBD would be expected to further improve its capabilities.

Overall, the potential applications of SPM in biomolecular research are promising, encompassing areas, such as drug discovery, protein engineering, and bio-nanotechnology. With continued advancements in SPM technology, the probing of biomolecules will lead to new insights and breakthroughs in understanding the structure and function of biomolecules.

ACKNOWLEDGMENTS

The authors thank the financial support of the Beijing Natural Science Foundation (Nos. Z190006 and 4192054), National Key Research and Development Program of China (Nos. 2019YFA0308000, 2020YFA0308800, and 2021YFA1400100), National Natural Science Foundation of China (Nos. 92163206, 61971035, 61725107, and 62271048), and the Strategic Priority Research Program of Chinese Academy of Sciences (No. XDB30000000).

CONFLICT OF INTEREST STATEMENT

The authors declare no conflict of interest.

ORCID

Cesare Grazioli http://orcid.org/0000-0002-6255-2041
Yeliang Wang http://orcid.org/0000-0002-8896-0748

REFERENCES

[1] Müller JB, Geyer PE, Colaço AR, et al. The proteome landscape of the kingdoms of life. *Nature*. 2020;582:592-596.
[2] Anggara K, Zhu Y, Delbianco M, et al. Exploring the molecular conformation space by soft molecule-surface collision. *J Am Chem Soc*. 2020;142:21420-21427.
[3] Abyzov A, Blackledge M, Zweckstetter M. Conformational dynamics of intrinsically disordered proteins regulate biomolecular condensate chemistry. *Chem Rev*. 2022;122:6719-6748.
[4] Hendry E, Carpy T, Johnston J, et al. Ultrasensitive detection and characterization of biomolecules using superchiral fields. *Nat Nanotechnol*. 2010;5:783-787.
[5] Leung C, Kinns H, Hoogenboom BW, Howorka S, Mesquida P. Imaging surface charges of individual biomolecules. *Nano Lett*. 2009;9:2769-2773.
[6] Labib M, Sargent EH, Kelley SO. Electrochemical methods for the analysis of clinically relevant biomolecules. *Chem Rev*. 2016;116:9001-9090.
[7] Maxwell DJ, Taylor JR, Nie S. Self-assembled nanoparticle probes for recognition and detection of biomolecules. *J Am Chem Soc*. 2002;124:9606-9612.
[8] Maruani A, Richards DA, Chudasama V. Dual modification of biomolecules. *Org Biomol Chem*. 2016;14:6165-6178.
[9] Lavery R, Lebrun A, Allemand JF, Bensimon D, Croquette V. Structure and mechanics of single biomolecules: experiment and simulation. *J Phys Condens Matter*. 2002;14:R383-R414.
[10] Kumar S, Li MS. Biomolecules under mechanical force. *Phys Rep*. 2010;486:1-74.
[11] Zhang Y, Ptacin JL, Fischer EC, et al. A semi-synthetic organism that stores and retrieves increased genetic information. *Nature*. 2017;551:644-647.
[12] Im J, Biswas S, Liu H, et al. Electronic single-molecule identification of carbohydrate isomers by recognition tunnelling. *Nat Commun*. 2016;7:13868.
[13] Longchamp JN, Rauschenbach S, Abb S, et al. Imaging proteins at the single-molecule level. *Proc Natl Acad Sci*. 2017;114:1474-1479.
[14] Lerner E, Cordes T, Ingargiola A, et al. Toward dynamic structural biology: two decades of single-molecule Förster resonance energy transfer. *Science*. 2018;359:1-12.
[15] Sahare S, Ghoderao P, Chan Y, Lee SL. Surface supramolecular assemblies tailored by chemical/physical and synergistic stimuli: a scanning tunneling microscopy study. *Nanoscale*. 2023;15:1981-2002.
[16] Lin JS, Tian XD, Li G, Zhang FL, Wang Y, Li JF. Advanced plasmonic technologies for multi-scale biomedical imaging. *Chem Soc Rev*. 2022;51:9445-9468.
[17] Zhai R, Fang B, Lai Y, et al. Small-molecule fluorogenic probes for mitochondrial nanoscale imaging. *Chem Soc Rev*. 2023;52:942-972.
[18] Miller A, Chia S, Toprakcioglu Z, et al. Enhanced surface nanoanalytics of transient biomolecular processes. *Sci Adv*. 2023;9:eabq3151.
[19] Dufrêne YF, Ando T, Garcia R, et al. Imaging modes of atomic force microscopy for application in molecular and cell biology. *Nat Nanotechnol*. 2017;12:295-307.
[20] Ido S, Kimura K, Oyabu N, et al. Beyond the helix pitch: direct visualization of native DNA in aqueous solution. *ACS Nano*. 2013;7:1817-1822.
[21] lundell TLB. Celebrating structural biology. *Nat Struct Mol Biol*. 2011;18:1304-1316.
[22] Martín Romano JC, Casado Aguilar P, Vázquez de Parga AL, et al. Interaction of chiral L-dialanine with Cu(100). *Phys Chem Chem Phys*. 2022;24:8022-8031.
[23] Kershner RJ, Bozano LD, Micheel CM, et al. Placement and orientation of individual DNA shapes on lithographically patterned surfaces. *Nat Nanotechnol*. 2009;4:557-561.
[24] Abb S, Harnau L, Gutzler R, Rauschenbach S, Kern K. Two-dimensional honeycomb network through sequence-controlled self-assembly of oligopeptides. *Nat Commun*. 2016;7:10335.
[25] Zheng Y, Yu L, Zou Y, Yang Y, Wang C. Steric dependence of chirality effect in surface-mediated peptide assemblies identified with scanning tunneling microscopy. *Nano Lett*. 2019;19:5403-5409.

2767441x, 0, Downloaded from https://onlinelibrary.wiley.com/doi/10.1002/idm2.12106 by CNR GROUP II Istituto di Scienza dell', Wiley Online Library on [26/06/2023]. See the Terms and Conditions (https://onlinelibrary.wiley.com/terms-and-conditions) on Wiley Online Library for rules of use; OA articles are governed by the applicable Creative Commons License

[26] Chen Q, Richardson NV. Enantiomeric interactions between nucleic acid bases and amino acids on solid surfaces. *Nat Mater*. 2003;2(5):324-328.
[27] Shapir E, Cohen H, Calzolari A, et al. Electronic structure of single DNA molecules resolved by transverse scanning tunnelling spectroscopy. *Nat Mater*. 2008;7:68-74.
[28] Wu X, Delbianco M, Anggara K, et al. Imaging single glycans. *Nature*. 2020;582:375-378.
[29] Rauschenbach S, Ternes M, Harnau L, Kern K. Mass spectrometry as a preparative tool for the surface science of large molecules. *Annu Rev Anal Chem*. 2016;9:473-498.
[30] Pappas CG, Shafi R, Sasselli IR, et al. Dynamic peptide libraries for the discovery of supramolecular nanomaterials. *Nat Nanotechnol*. 2016;11:960-967.
[31] Baier C, Stimming U. Imaging single enzyme molecules under in situ conditions. *Angew Chem Int Ed*. 2009;48:5542-5544.
[32] Pavliček N, Gross L. Generation, manipulation and characterization of molecules by atomic force microscopy. *Nat Rev Chem*. 2017;1:0005.
[33] Alsteens D, Gaub HE, Newton R, Pfreundschuh M, Gerber C, Müller DJ. Atomic force microscopy-based characterization and design of biointerfaces. *Nat Rev Mater*. 2017;2:17008.
[34] Kühnle A, Linderoth TR, Hammer B, Besenbacher F. Chiral recognition in dimerization of adsorbed cysteine observed by scanning tunnelling microscopy. *Nature*. 2002;415:891-893.
[35] Adamcik J, Jung JM, Flakowski J, De Los Rios P, Dietler G, Mezzenga R. Understanding amyloid aggregation by statistical analysis of atomic force microscopy images. *Nat Nanotechnol*. 2010;5:423-428.
[36] Rodríguez-Galván A, Contreras-Torres FF. Scanning tunneling microscopy of biological structures: an elusive goal for many years. *Nanomaterials*. 2022;12:3013.
[37] Smith DP, Bryant A, Quate CF, Rabe JP, Gerber C, Swalen JD. Images of a lipid bilayer at molecular resolution by scanning tunneling microscopy. *Proc Natl Acad Sci*. 1987;84:969-972.
[38] Wang L, Song Y, Han X, Zhang B, Wang E. Growth of cationic lipid toward bilayer lipid membrane by solution spreading: scanning probe microscopy study. *Chem Phys Lipids*. 2003;123:177-185.
[39] Binnig G, Rohrer H, Gerber C, Weibel E. Tunneling through a controllable vacuum gap. *Appl Phys Lett*. 1982;40:178-180.
[40] Kano S, Tada T, Majima Y. Nanoparticle characterization based on STM and STS. *Chem Soc Rev*. 2015;44:970-987.
[41] Diller K, Papageorgiou AC, Klappenberger F, Allegretti F, Barth JV, Auwärter W. In vacuo interfacial tetrapyrrole metallation. *Chem Soc Rev*. 2016;45:1629-1656.
[42] Gerber C, Lang HP. How the doors to the nanoworld were opened. *Nat Nanotechnol*. 2006;1:3-5.
[43] Sugimoto Y, Abe M, Hirayama S, Oyabu N, Custance Ó, Morita S. Atom inlays performed at room temperature using atomic force microscopy. *Nat Mater*. 2005;4:156-159.
[44] Jiang W, Pacella MS, Athanasiadou D, et al. Chiral acidic amino acids induce chiral hierarchical structure in calcium carbonate. *Nat Commun*. 2017;8:15066.
[45] Preiner J, Horner A, Karner A, et al. High-speed AFM images of thermal motion provide stiffness map of interfacial membrane protein moieties. *Nano Lett*. 2015;15:759-763.
[46] Viani MB, Pietrasanta LI, Thompson JB, et al. Probing protein–protein interactions in real time. *Nature Struct Biol*. 2000;7:644-647.
[47] Simpson JD, Ray A, Koehler M, Mohammed D, Alsteens D. Atomic force microscopy applied to interrogate nanoscale cellular chemistry and supramolecular bond dynamics for biomedical applications. *Chem Commun*. 2022;58:5072-5087.
[48] Guo J, Jiang Y. Submolecular insights into interfacial water by hydrogen-sensitive scanning probe microscopy. *Acc Chem Res*. 2022;55:1680-1692.
[49] Chan FY, Kurosaki R, Ganser C, Takeda T, Uchihashi T. Tip-scan high-speed atomic force microscopy with a uniaxial substrate stretching device for studying dynamics of biomolecules under mechanical stress. *Rev Sci Instrum*. 2022;93:113703.
[50] Xing P, Li Y, Xue S, et al. Occurrence of chiral nanostructures induced by multiple hydrogen bonds. *J Am Chem Soc*. 2019;141:9946-9954.
[51] Rothemund PWK. Folding DNA to create nanoscale shapes and patterns. *Nature*. 2006;440:297-302.
[52] Heo C, Ha T, You C, et al. Identifying fibrillization state of Aβ protein via near-field THz conductance measurement. *ACS Nano*. 2020;14:6548-6558.
[53] Pyles H, Zhang S, De Yoreo JJ, Baker D. Controlling protein assembly on inorganic crystals through designed protein interfaces. *Nature*. 2019;571:251-256.
[54] Gross L, Schuler B, Pavliček N, et al. Atomic force microscopy for molecular structure elucidation. *Angew Chem Int Ed*. 2018;57:3888-3908.
[55] Garcia R, Herruzo ET. The emergence of multifrequency force microscopy. *Nat Nanotechnol*. 2012;7:217-226.
[56] Ido S, Kimiya H, Kobayashi K, Kominami H, Matsushige K, Yamada H. Immunoactive two-dimensional self-assembly of monoclonal antibodies in aqueous solution revealed by atomic force microscopy. *Nat Mater*. 2014;13:264-270.
[57] Cartagena A, Hernando-Pérez M, Carrascosa JL, de Pablo PJ, Raman A. Mapping in vitro local material properties of intact and disrupted virions at high resolution using multi-harmonic atomic force microscopy. *Nanoscale*. 2013;5:4729-4736.
[58] Herruzo ET, Asakawa H, Fukuma T, Garcia R. Three-dimensional quantitative force maps in liquid with 10 piconewton, angstrom and sub-minute resolutions. *Nanoscale*. 2013;5:2678-2685.
[59] Albrecht TR, Grütter P, Horne D, Rugar D. Frequency modulation detection using high-Q cantilevers for enhanced force microscope sensitivity. *J Appl Phys*. 1991;69:668-673.
[60] Rinke G, Rauschenbach S, Schrettl S, et al. Soft-landing electrospray ion beam deposition of sensitive oligoynes on surfaces in vacuum. *Int J Mass Spectrom*. 2015;377:228-234.
[61] Driscoll RJ, Youngquist MG, Baldeschwieler JD. Atomic-scale imaging of DNA using scanning tunnelling microscopy. *Nature*. 1990;346:294-296.
[62] Guo Y, Hou J, Zhang X, Yang Y, Wang C. Stabilization effect of amino acid side chains in peptide assemblies on graphite studied by scanning tunneling microscopy. *Chem Phys Chem*. 2017;18:926-934.

2767441x, 0, Downloaded from https://onlinelibrary.wiley.com/doi/10.1002/idm2.12106 by CNR GROUP II Istituto di Scienza dell', Wiley Online Library on [26/06/2023]. See the Terms and Conditions (https://onlinelibrary.wiley.com/terms-and-conditions) on Wiley Online Library for rules of use; OA articles are governed by the applicable Creative Commons License

[63] Cricenti A, Selci S, Felici AC, et al. Molecular structure of DNA by scanning tunneling microscopy. *Science*. 1989;245: 1226-1227.
[64] Pawlak R, Vilhena JG, Hinaut A, et al. Conformations and cryo-force spectroscopy of spray-deposited single-strand DNA on gold. *Nat Commun*. 2019;10:685.
[65] Tanaka H, Kawai T. Partial sequencing of a single DNA molecule with a scanning tunnelling microscope. *Nat Nanotechnol*. 2009;4:518-522.
[66] Tanaka H, Taniguchi M. Sequencing of adenine in DNA by scanning tunneling microscopy. *Jpn J Appl Phys*. 2017; 56:08LB02.
[67] Leung C, Bestembayeva A, Thorogate R, et al. Atomic force microscopy with nanoscale cantilevers resolves different structural conformations of the DNA double helix. *Nano Lett*. 2012;12:3846-3850.
[68] Lee AJ, Szymonik M, Hobbs JK, Wälti C. Tuning the translational freedom of DNA for high speed AFM. *Nano Res*. 2015;8:1811-1821.
[69] Nievergelt AP, Kammer C, Brillard C, et al. Large-range HS-AFM imaging of DNA self-assembly through in situ data-driven control. *Small Methods*. 2019;3:1900031.
[70] Aghebat Rafat A, Sagredo S, Thalhammer M, Simmel FC. Barcoded DNA origami structures for multiplexed optimization and enrichment of DNA-based protein-binding cavities. *Nat Chem*. 2020;12:852-859.
[71] Li W, Jin J, Liu X, Wang L. Structural transformation of guanine coordination motifs in water induced by metal ions and temperature. *Langmuir*. 2018;34:8092-8098.
[72] Azhati A, Han L, Qu Z, et al. Insight on metal ions inducing chiral self-assembly of DNA in silica mineralization. *Nano Res*. 2022;175:12274.
[73] Xu D, Dong M, Rauls E, Otero R, Linderoth TR, Besenbacher F. Coadsorption of guanine and cytosine on graphite: ordered structure based on GC pairing. *Nano Lett*. 2006;6:1434-1438.
[74] Mamdouh W, Dong M, Xu S, Rauls E, Besenbacher F. Supramolecular nanopatterns self-assembled by adenine–thymine quartets at the liquid/solid interface. *J Am Chem Soc*. 2006;128:13305-13311.
[75] Ciesielski A, Lena S, Masiero S, Spada GP, Samorì P. Dynamers at the solid–liquid interface: controlling the reversible assembly/reassembly process between two highly ordered supramolecular guanine motifs. *Angew Chem Int Ed*. 2010;49:1963-1966.
[76] Zhang C, Xie L, Ding Y, Xu W. Scission and stitching of adenine structures by water molecules. *Chem Commun*. 2018;54:771-774.
[77] Eralp T, Shavorskiy A, Zheleva ZV, et al. Global and local expression of chirality in serine on the Cu{110} surface. *Langmuir*. 2010;26:18841-18851.
[78] Barlow S, Raval R. Nanoscale insights in the creation and transfer of chirality in amino acid monolayers at defined metal surfaces. *Curr Opin Colloid Interface Sci*. 2008;13: 65-73.
[79] Xu LP, Liu Y, Zhang X. Interfacial self-assembly of amino acids and peptides: scanning tunneling microscopy investigation. *Nanoscale*. 2011;3:4901-4915.
[80] Smerieri M, Vattuone L, Kravchuk T, Costa D, Savio L. (S)-glutamic acid on Ag(100): self-assembly in the nonzwitterionic form. *Langmuir*. 2011;27:2393-2404.
[81] Tranca I, Smerieri M, Savio L, Vattuone L, Costa D, Tielens F. Unraveling the self-assembly of the (*S*)-glutamic acid "flower" structure on Ag(100). *Langmuir*. 2013;29: 7876-7884.
[82] Forster M, Dyer MS, Persson M, Raval R. 2D random organization of racemic amino acid monolayers driven by nanoscale adsorption footprints: proline on Cu(110). *Angew Chem Int Ed*. 2010;49:2344-2348.
[83] Wang M, Zhou P, Wang J, et al. Left or right: how does amino acid chirality affect the handedness of nanostructures self-assembled from short amphiphilic peptides? *J Am Chem Soc*. 2017;139:4185-4194.
[84] Xing Q, Zhang J, Xie Y, et al. Aromatic motifs dictate nanohelix handedness of tripeptides. *ACS Nano*. 2018;12: 12305-12314.
[85] Kodera N, Yamamoto D, Ishikawa R, Ando T. Video imaging of walking myosin V by high-speed atomic force microscopy. *Nature*. 2010;468:72-76.
[86] Della Pia EA, Chi Q, Macdonald JE, Ulstrup J, Jones DD, Elliott M. Fast electron transfer through a single molecule natively structured redox protein. *Nanoscale*. 2012;4: 7106-7113.
[87] Liu L, Zhang L, Mao X, Niu L, Yang Y, Wang C. Chaperon-mediated single molecular approach toward modulating Aβ peptide aggregation. *Nano Lett*. 2009;9:4066-4072.
[88] Qu F, Yu L, Xie H, et al. Studies on composition and sequence effects in surface-mediated octapeptide assemblies by using scanning tunneling microscopy. *J Phys Chem C*. 2017;121:10364-10369.
[89] Ha NTN, Sharma A, Slawig D, et al. Charge-ordered α-helical polypeptide monolayers on Au(111). *J Phys Chem C*. 2020;124:5734-5739.
[90] Nguyen TNH, Xue S, Tegenkamp C. Heterochiral dimer formation of α-L- and α-D-polyalanine molecules on surfaces. *J Phys Chem C*. 2020;124:11075-11080.
[91] Mao XB, Wang CX, Wu XK, et al. Beta structure motifs of islet amyloid polypeptides identified through surface-mediated assemblies. *Proc Natl Acad Sci*. 2011;108: 19605-19610.
[92] Kalashnyk N, Nielsen JT, Nielsen EH, et al. Scanning tunneling microscopy reveals single-molecule insights into the self-assembly of amyloid fibrils. *ACS Nano*. 2012;6: 6882-6889.
[93] Lingenfelder M, Tomba G, Costantini G, Colombi Ciacchi L, De Vita A, Kern K. Tracking the chiral recognition of adsorbed dipeptides at the single-molecule level. *Angew Chem*. 2007;119:4576-4579.
[94] Li Y, Liu C, Xie Y, et al. Single-molecule observation of the K(+)-induced switching of valinomycin within a template network. *Chem Commun*. 2013;49:9021-9023.
[95] Morange M. What history tells us. XXVII. A new life for allostery. *J Biosci*. 2012;37:13-17.
[96] Chen Y, Nie H, Deng K, et al. Peptide recognition by functional supramolecular nanopores with complementary size and binding sites. *Nano Res*. 2016;9:1452-1459.

2767441x, 0, Downloaded from https://onlinelibrary.wiley.com/doi/10.1002/idm2.12106 by CNR GROUP II Istituto di Scienza dell', Wiley Online Library on [26/06/2023]. See the Terms and Conditions (https://onlinelibrary.wiley.com/terms-and-conditions) on Wiley Online Library for rules of use; OA articles are governed by the applicable Creative Commons License

[97] Rubinov B, Wagner N, Matmor M, Regev O, Ashkenasy N, Ashkenasy G. Transient fibril structures facilitating non-enzymatic self-replication. *ACS Nano*. 2012;6:7893-7901.
[98] Meirzadeh E, Sapir L, Cohen H, et al. Nonclassical crystal growth as explanation for the riddle of polarity in centrosymmetric glycine crystals. *J Am Chem Soc*. 2016;138:14756-14763.
[99] Jacobs J, Pavlović D, Prydderch H, et al. Polypeptide nanoparticles obtained from emulsion polymerization of amino acid *N*-carboxyanhydrides. *J Am Chem Soc*. 2019;141:12522-12526.
[100] So CR, Hayamizu Y, Yazici H, et al. Controlling self-assembly of engineered peptides on graphite by rational mutation. *ACS Nano*. 2012;6:1648-1656.
[101] Baneyx F, Mujacic M. Recombinant protein folding and misfolding in *Escherichia coli*. *Nature Biotechnol*. 2004;22:1399-1408.
[102] Joachim C, Gimzewski JK, Aviram A. Electronics using hybrid-molecular and mono-molecular devices. *Nature*. 2000;408:541-548.
[103] Hofmann J, Hahm HS, Seeberger PH, Pagel K. Identification of carbohydrate anomers using ion mobility–mass spectrometry. *Nature*. 2015;526:241-244.
[104] Gray CJ, Migas LG, Barran PE, et al. Advancing solutions to the carbohydrate sequencing challenge. *J Am Chem Soc*. 2019;141:14463-14479.
[105] Zhuravel R, Stern A, Fardian-Melamed N, et al. Advances in synthesis and measurement of charge transport in DNA-based derivatives. *Adv Mater*. 2018;30:1706984.
[106] Rauschenbach S, Vogelgesang R, Malinowski N, et al. Electrospray ion beam deposition: soft-landing and fragmentation of functional molecules at solid surfaces. *ACS Nano*. 2009;3:2901-2910.
[107] Rauschenbach S, Stadler FL, Lunedei E, et al. Electrospray ion beam deposition of clusters and biomolecules. *Small*. 2006;2:540-547.
[108] Volný M, Tureček F. High efficiency in soft landing of biomolecular ions on a plasma-treated metal surface: are double-digit yields possible? *J Mass Spectrom*. 2006;41:124-126.
[109] Gologan B, Takáts Z, Alvarez J, et al. Ion soft-landing into liquids: protein identification, separation, and purification with retention of biological activity. *J Am Soc Mass Spectrom*. 2004;15:1874-1884.
[110] Volný M, Sengupta A, Wilson CB, Swanson BD, Davis EJ, Tureček F. Surface-enhanced Raman spectroscopy of soft-landed polyatomic ions and molecules. *Anal Chem*. 2007;79:4543-4551.
[111] Hekimi S, Guarente L. Genetics and the specificity of the aging process. *Science*. 2003;299:1351-1354.
[112] Hadjar O, Wang P, Futrell JH, Laskin J. Effect of the surface on charge reduction and desorption kinetics of soft landed peptide ions. *J Am Soc Mass Spectrom*. 2009;20:901-906.
[113] Volný M, Elam WT, Branca A, Ratner BD, Tureček F. Preparative soft and reactive landing of multiply charged protein ions on a plasma-treated metal surface. *Anal Chem*. 2005;77:4890-4896.
[114] Shang L, Dong S, Nienhaus GU. Ultra-small fluorescent metal nanoclusters: synthesis and biological applications. *Nano Today*. 2011;6:401-418.
[115] Ochner H, Szilagyi S, Edte M, Malavolti L, Rauschenbach S, Kern K. Phase reconstruction of low-energy electron holograms of individual proteins. *ACS Nano*. 2022;16:18568-18578.
[116] Klemm D, Heublein B, Fink HP, Bohn A. Cellulose: fascinating biopolymer and sustainable raw material. *Angew Chem Int Ed*. 2005;44:3358-3393.
[117] Klemm D, Heublein B, Fink H-P, Bohn A. Cellulose: faszinierendes Biopolymer und nachhaltiger Rohstoff. *Angew Chem*. 2005;117:3422-3458.
[118] Mucha E, González Flórez AI, Marianski M, et al. Glycan fingerprinting via cold-ion infrared spectroscopy. *Angew Chem Int Ed*. 2017;56:11248-11251.
[119] Molinari M. *N*-glycan structure dictates extension of protein folding or onset of disposal. *Nat Chem Biol*. 2007;3:313-320.
[120] Anggara K, Zhu Y, Fittolani G, et al. Identifying the origin of local flexibility in a carbohydrate polymer. *Proc Natl Acad Sci*. 2021;118:e2102168118.
[121] Nagase H, Ogawa N, Endo T, Shiro M, Ueda H, Sakurai M. Crystal structure of an anhydrous form of trehalose: structure of water channels of trehalose polymorphism. *J Phys Chem B*. 2008;112:9105-9111.
[122] Elbein AD. New insights on trehalose: a multifunctional molecule. *Glycobiology*. 2003;13:17R-27R.
[123] Tanaka K, Kawamura M, Otake K, et al. Trehalose does not affect the functions of human neutrophils in vitro. *Surg Today*. 2014;44:332-339.
[124] Abb S, Tarrat N, Cortés J, et al. Polymorphism in carbohydrate self-assembly at surfaces: STM imaging and theoretical modelling of trehalose on Cu(100). *RSC Adv*. 2019;9:35813-35819.
[125] Abb S, Tarrat N, Cortés J, et al. Carbohydrate self-assembly at surfaces: STM imaging of sucrose conformation and ordering on Cu(100). *Angew Chem Int Ed*. 2019;58:8336-8340.
[126] Guberman M, Seeberger PH. Automated glycan assembly: a perspective. *J Am Chem Soc*. 2019;141:5581-5592.
[127] Seeberger PH. The logic of automated glycan assembly. *Acc Chem Res*. 2015;48:1450-1463.
[128] Panza M, Pistorio SG, Stine KJ, Demchenko AV. Automated chemical oligosaccharide synthesis: novel approach to traditional challenges. *Chem Rev*. 2018;118:8105-8150.
[129] Solís D, Bovin NV, Davis AP, et al. A guide into glycosciences: how chemistry, biochemistry and biology cooperate to crack the sugar code. *Biochim Biophys Acta (BBA)—Gen Subj*. 2015;1850:186-235.
[130] Seo J, Hoffmann W, Warnke S, et al. An infrared spectroscopy approach to follow β-sheet formation in peptide amyloid assemblies. *Nat Chem*. 2017;9:39-44.
[131] Cocinero EJ, Carcabal P, Vaden TD, Simons JP, Davis BG. Sensing the anomeric effect in a solvent-free environment. *Nature*. 2011;469:76-79.
[132] Ingram AJ, Boeser CL, Zare RN. Going beyond electrospray: mass spectrometric studies of chemical reactions in and on liquids. *Chem Sci*. 2016;7:39-55.

2767441x, 0, Downloaded from https://onlinelibrary.wiley.com/doi/10.1002/idm2.12106 by CNR GROUP II Istituto di Scienza dell', Wiley Online Library on [26/06/2023]. See the Terms and Conditions (https://onlinelibrary.wiley.com/terms-and-conditions) on Wiley Online Library for rules of use; OA articles are governed by the applicable Creative Commons License

AUTHOR BIOGRAPHIES

Baofei Hou is currently a doctoral student at the School of Integrated Circuits and Electronics (SICE), Beijing Institute of Technology (BIT), under the supervision of Prof. Yeliang Wang. His research focuses on investigating the properties of organic molecules and transition metal dichalcogenides using scanning tunneling microscopy (STM).

Teng Zhang completed his PhD at Uppsala University and later joined Prof. Yeliang Wang's group at the Beijing Institute of Technology as an Assistant Professor in 2018. His research interests cover the design, fabrication, and characterization of low-dimensional functional structures.

Xu Wu obtained his BS from Nankai University and PhD from the Institute of Physics (IOP), Chinese Academy of Sciences (CAS). He conducted research as a Humboldt Fellow scientist at the Max-Planck-Institute for Solid Research in Germany before joining BIT as a professor in 2021. His current research interest is the study of single big biomolecules with the combination of electrospray ion beam deposition and low-temperature STM.

Yeliang Wang obtained his BS and MS degrees from Wuhan University of Technology and PhD degree from IOP, CAS. He then joined in the Max-Planck-Institute for Solid Research, Germany, as a Humboldt Fellow. He was appointed associate professor in 2008 and full professor in 2013 at IOP, CAS. He was honored with the National Science Fund for Distinguished Young Scholars (2017). Currently, he is a full professor, Director of the MIIT Key Laboratory for Low-Dimensional Quantum Structure and Devices and Dean of SICE at BIT. His research interest is the study and application of new electronic materials and devices.

How to cite this article: Hou B, Zhang T, Yang H, et al. Advances in probing single biomolecules: from DNA bases to glycans. *Interdiscip Mater*. 2023;1-18. doi:10.1002/idm2.12106

2767441x, 0, Downloaded from https://onlinelibrary.wiley.com/doi/10.1002/idm2.12106 by CNR GROUP II Istituto di Scienza dell', Wiley Online Library on [26/06/2023]. See the Terms and Conditions (https://onlinelibrary.wiley.com/terms-and-conditions) on Wiley Online Library for rules of use; OA articles are governed by the applicable Creative Commons License